Academic Journal of Science and Technology
ISSN: 2771-3032 | Vol. 19, No. 1, 2026

A Scheduling Optimization Approach for Heterogeneous Feeder Container Fleet with User Timeliness Satisfaction

Jun Jiang *, **Mingjie Li**

School of Navigation and Shipping, Shandong Jiaotong University, Weihai Shandong, 264209, China

* **Corresponding author**: Jun Jiang (Email: junjiangsdjtu@163.com)

Abstract: Against the background of global trade expansion and the shipping industry's low-carbon transition, feeder transportation faces challenges in delivery timeliness and scheduling heterogeneous fleets composed of vessels powered by different fuel types. To address this issue, this study takes oil-fueled feeder container ships (OFSs) and LNG-fueled feeder container ships (LFSs) as examples to investigate the impact of actual cargo delivery times on users' irrational psychological behaviors, as well as to propose solutions for heterogeneous feeder fleet scheduling problems. Specifically, the main contributions of this research are as follows. Firstly, a heterogeneous feeder container fleet operation strategy is proposed, integrating OFSs and LFSs to reduce carbon emissions and enhance operational efficiency. Secondly, an optimization model of heterogeneous feeder container fleet with user timeliness satisfaction (HFCF-UTS) is constructed. This model quantitatively measures user timeliness satisfaction by combining prospect theory and fuzzy time windows. Thirdly, an adaptive single-valued neutrosophic large neighborhood search (ASVNLNS) algorithm is designed. This algorithm adopts single-valued neutrosophic sets (SvNSs) and an improved utility function to update the operator scoring mechanism and ultimately achieve rationalized operator scoring. Finally, based on the real operation data of a Norwegian shipping company, the calculation results show that the proposed algorithm reasonably improves the user timeliness satisfaction and reduces the total turnaround cost, outperforming the adaptive large neighborhood search algorithm.

Keywords: User Timeliness Satisfaction; Heterogeneous Fleet; Feeder Container Ships; Ship Scheduling; Adaptive Single-valued Veutrosophic Large Neighborhood Search Algorithm.

1. Introduction

With the continuous development of the global economy, the shipping industry has undertaken over 80 percent of global trade cargo, serving as the primary mode of transportation for international trade [1]. Against this backdrop, the status and role of feeder shipping lines in maritime transport have become increasingly prominent, and their containerization and feeder networks have developed significantly [2,3]. However, feeder transportation is highly susceptible to interference from factors such as meteorological conditions, sea conditions, and port congestion, resulting in low transport efficiency and delays in cargo arrival. This not only increases the operating cost of feeder shipping lines, but also shapes users' expectations regarding delivery timeliness due to prolonged transportation times, thereby reducing their service experience and satisfaction.

Meanwhile, a multitude of maritime trade has also exacerbated the issue of greenhouse gas emissions from ships, among which carbon dioxide (CO_2) emissions have accounted for more than 3% of global total emissions [4]. To address this issue, the International Maritime Organization implemented a series of resolutions between 2022 and 2023 to encourage the application of low-carbon fuels and reduce greenhouse gas emissions [5]. Correspondingly, many feeder shipping lines have gradually selected Liquefied Natural Gas (LNG) as an alternative fuel and adopted LNG-fueled feeder container ships (LFSs) to replace oil-fueled feeder container ships (OFSs), aiming to reduce CO_2 emissions. Nevertheless, LFSs are difficult to fully replace OFSs in the short term, and conventional OFSs are expected to remain in service for a considerable period. Therefore, in the specific context of feeder container ship scheduling, this study takes the user demand timeliness as the entry point and investigates how to schedule a heterogeneous feeder container fleet (OFSs and LFSs) to maximize user timeliness satisfaction and minimize turnaround cost. This problem is refined and formulated as an optimization model of a heterogeneous feeder container fleet with user timeliness satisfaction (HFCF-UTS). Additionally, this study provides relevant research literature on ship scheduling, delivery timeliness, and the adaptive large neighborhood search algorithm (ALNS) to better explore the HFCF-UTS model.

In the ship scheduling aspect, the primary aim of ship scheduling is to plan the routes, port calling sequences, berth allocation, and sailing schedules of given ships under different transportation tasks [6-10]. Moreover, based on the homogeneous fleet, researchers have proposed the heterogeneous fleet scheduling problem and conducted extensive studies. For example, Dulebenets [11] first proposed a novel heterogeneous fleet scheduling model and verified the effectiveness of this model through numerical experiments. Pasha et al. [12] proposed an optimization model integrating all liner shipping decisions for the problem of heterogeneous fleet scheduling on different routes. Zhao et al. [13] first incorporated the heterogeneity of container ships and the uncertainty of ship scheduling into a unified framework and developed a two-step method with two programming sub-models. Du et al. [14] innovatively designed a heterogeneous fleet deployment and scheduling model, which effectively applies different green technologies to reduce sulfur or carbon emissions from container ships. Wang et al. [15] proposed a mixed-integer nonlinear model to successfully solve the optimization problems of heterogeneous ship fleet co-management.

In the delivery timeliness aspect, the quality of on-time delivery significantly influences users' service perception, which in turn affects an enterprise's reputation and the quality of its decision-making [16]. Therefore, a lot of researchers have proposed various approaches to ensure delivery timeliness and enhance user satisfaction. For example, Liang et al. [17] developed a bi-objective vehicle routing model with multiple time periods, aiming to minimize the deterioration of perishable freshness and improve customer satisfaction. Huang et al. [18] developed a distribution programming model for fresh products by incorporating time-satisfaction and quality-satisfaction functions, which provides actionable insights for distributors to improve delivery punctuality and optimize the customer experience. Yu et al. [19] integrated customer satisfaction and carbon emissions into a unified framework for the last-mile delivery problem and proposed two last-mile delivery models. Seo and Roh [20] proposed a forward-looking evaluation framework to systematically measure the online and offline satisfaction of consumers in the food delivery industry, providing some valuable insight. For the issue of timely delivery in hilly areas, Maji et al. [21] developed a multi-objective multipath delivery mode, which effectively reduces delivery times and improves customer satisfaction.

In the ALNS algorithm aspect, Ropke and Pisinger [22] first proposed the ALNS algorithm in 2006 to solve the vehicle routing problem and its variants. Subsequently, many scholars proposed various improved or enhanced ALNS algorithms to address practical problems in different fields. For example, Wang et al. [23] integrated a feasibility check method into the ALNS algorithm to handle the tugboat scheduling problem. Wang et al. [24] proposed an ALNS algorithm by intermixing a hybrid multi-start mechanism and a local search algorithm to address the pilotage plan problem. Zhang et al. [25] proposed a two-phase ALNS that integrates extended binary particle swarm optimization and a local search algorithm to solve the electric location routing problem. Gao et al. [26] innovatively introduced a metaheuristic optimization strategy into the ALNS algorithm, effectively enhancing solution quality and significantly reducing the computational time. Özkır and Coban [27] tailored an ALNS algorithm for solving the route problem of multi-load automated guided vehicles, and applied it in a case of a refrigerator factory.

In summary, many researchers have comprehensively considered the impacts of environment, cost, and user satisfaction on the ship scheduling and timeliness distribution, and conducted relatively specific studies. However, the aforementioned research fails to account for the influence of user timeliness satisfaction on heterogeneous feeder container fleet scheduling. Therefore, this study proposes a novel ship scheduling method tailored for a heterogeneous feeder container fleet. The main contributions are summarized as follows.

First, an operational mode of a heterogeneous feeder container fleet is constructed by incorporating LFSs into the feeder transportation system to overcome limitations of traditional single-type ship operation and reduce carbon emissions.

Second, a bi-objective mixed-integer nonlinear programming model for HFCF-UTS is proposed, which introduces prospect theory and fuzzy time windows to quantify user timeliness satisfaction and enhance it under the premise of total turnaround cost minimization.

Third, an adaptive single-valued neutrosophic large neighborhood search (ASVNLNS) algorithm is developed, which integrates single-valued neutrosophic sets (SvNSs) and improved utility function into the operator scoring mechanism to reasonably quantify operator performance and assign scores.

The remainder of this study is organized as follows. Section 2 introduces the relevant knowledge and mathematical methods required. Section 3 indicates the studied problem and introduces the HFCF-UTS model. Section 4 designs a kind of ASVNLNS algorithm. Section 5 provides a series of numerical experiments to verify the rationality of the ASVNLNS algorithm and HFCF-UTS model. Section 6 gives a conclusion and further research prospects.

2. Preliminary Studies

For convenience, this study introduces relevant definitions of SvNSs, prospect theory, and fuzzy time windows to enhance understanding.

Definition 1 [28, 29]. Let X be a universal set. An SvNS N in X is given as

$$N=\left\{\left\langle x,T_N\left(x\right),I_N\left(x\right),F_N\left(x\right)\right\rangle \mid x\in X\right\}, \tag{1}$$

where, $T_N(x), I_N(x), F_N(x) \in [0,1]$ and $0 \le T_N(x) + I_N(x) + F_N(x) \le 3$. For convenience, a fundamental element $p = \langle T, I, F\rangle$ in N is called a single-valued neutrosophic number.

Definition 2 [30, 31]. Prospect theory is a theoretical framework for describing an individual's decision-making preferences in uncertain situations. This theory divides the results into gain and loss domains according to a reference point. In the gain domain, individuals typically exhibit risk aversion, preferring certain outcomes over risky alternatives with potentially higher returns. However, in the loss domain, individuals tend to display risk-seeking behavior to avoid certain losses. Moreover, under the same magnitude, the concept of loss aversion suggests that losses loom larger than gains. Therefore, the value function is introduced in prospect theory, which describes the individual's subjective perception of gains and losses, and is formed as

$$PT\left(q\right)=\begin{cases} q^{\alpha}, & q\ge 0; \\ -\lambda\left(-q\right)^{\beta}, & q<0, \end{cases} \tag{2}$$

where, $\alpha, \beta \in [0, 1]$ indicates the loss sensitivity; $\lambda > 1$ indicates the loss aversion degree.

Definition 3 [32, 33]. Fuzzy set theory is used to describe and process personal human feelings. More intuitively, the shipping line's service level $L(t)$ for each customer is defined by a fuzzy membership function and described as

$$L\left(t\right)=\begin{cases} 0, & t<EAT; \\ \Psi\left(t\right), & EAT\le t<ET; \\ 1, & ET\le t<LT; \\ \Upsilon\left(t\right), & LT\le t<LAT; \\ 0, & t\ge LAT. \end{cases} \tag{3}$$

Here, t is a service start time; $\Psi(t)$ is a non-decreasing function; $\Upsilon(t)$ is a non-increasing function, and $L(t) \in [0,1]$. Moreover, EAT is the earliest service time that a customer endured; LAT is the latest service time that a customer endured; ET is the earliest service time that a customer anticipated; LT is the latest service time that a customer anticipated. More detailed, if a customer is not served within $[EAT, LAT]$, the satisfaction level is 0. If a customer is served within $[ET, LT]$, the satisfaction level is 1. If a customer is served within $[EAT, ET]$ or $[LT, LAT]$, the satisfaction level is acceptable. Then, the fuzzy membership function of service time is shown in Figure. 1.

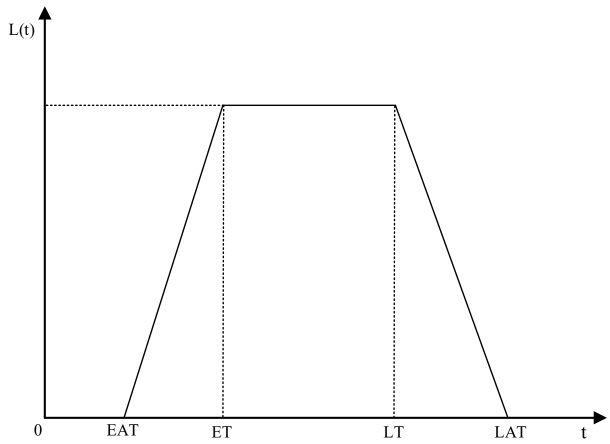

Figure 1. The fuzzy membership function of service time

3. Optimization Model

3.1. Problem Description

This study defines a feeder transportation network that comprises a given hub port, a group of feeder ports, and corresponding routes, while considering a heterogeneous feeder container fleet, as illustrated in Figure. 2. In detail, a shipping line typically operates multiple routes, each of which has a different port calling sequence. Meanwhile, let $R = \{1,2,3,\ldots,r\}$ denote the set of routes. Let $P_r = \{0,1,2,3,\ldots,p\}, r \in R$ denote the set of ports visited on route r, port 0 represents the hub port. Let $S_r = \{1,2,3,\ldots,s\}, r \in R$ denote the set of voyage legs on route r, and a voyage leg s is described as a pathway from port p to port $p+1$. For instance, the route 2 has 7 voyage legs. Otherwise, this study assumes the set of heterogeneous feeder container fleet is denoted as $K = K_1 \cup K_2 = \{1,2,3,\ldots,k_1,k_1+1,\ldots,k_1+k_2\}$. Among them, the OFS set is represented as $K_1 = \{1,2,3,\ldots,k_1\}$, LFS set is represented as $K_2 = \{k_1+1, k_1+2, k_1+3,\ldots,k_1+k_2\}$. For convenience, the model parameters and variables are shown in Table 1. Additionally, this study proposes a series of hypotheses to facilitate modeling.

(A1) The heterogeneous feeder container fleet departs from and returns to the hub port;

(A2) The feeder container ship is allowed to serve multiple ports, but each port is only served once;

(A3) The LFS is bunkered at a port equipped with bunkering facilities;

(A4) The total voyage of a feeder container ship on a route does not exceed the ship's endurance;

(A5) The feeder container ship employs an economical speed during navigation;

(A6) The LFS chose LNG as its marine fuel;

(A7) The prices of LNG and Low Sulfur Fuel Oil (LSFO) are unaffected by the marine fuel market and remain constant;

(A8) All feeder container ships are owned by the shipping line;

(A9) All cargoes are loaded in the Twenty-foot Equivalent Unit (TEU) container.

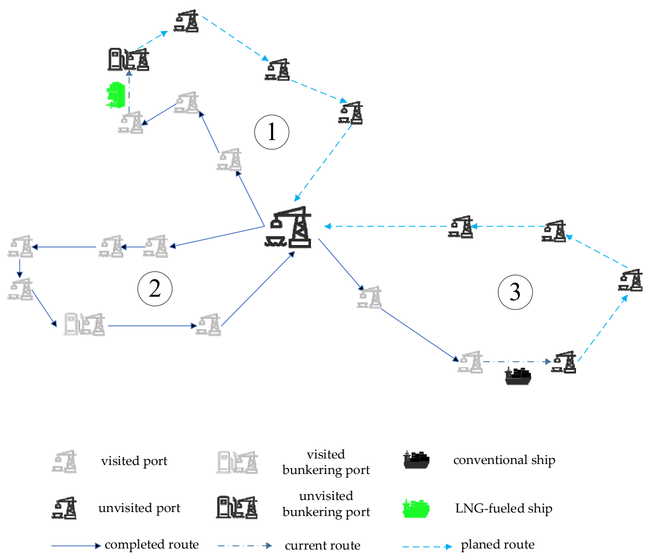

Figure 2. The feeder transportation network

3.2. Model Formulation for HFCF-UTS

This subsection proposes a bi-objective mixed-integer nonlinear programming model for HFCF-UTS problem, aiming to enhance the scheduling efficiency, reduce turnaround cost, and improve the timeliness of transportation services. Then, the main parts are as follows.

3.2.1. The Fixed Cost

During the operation period, the fixed cost of the heterogeneous feeder container fleet includes depreciation expense of ships, maintenance fees, insurance premiums, crew wages, and management fees [10], etc. Then, the determination of ship operation time is the key to calculating the fixed cost. For this purpose, this study calculates the sail time T_{rk}^{sail} of ship k on route r and the container handling time T_{rk}^{hand}, respectively. These calculation formulas are defined as

$$T_{rk}^{sail} = \sum_{r \in R} \sum_{s \in S_r} \frac{l_{rs}}{\bar{\upsilon}}, \forall k \in K, \tag{4}$$

$$T_{rk}^{hand} = \sum_{r \in R} \sum_{p \in P_r} \sum_{h_p \in H_{rp}} \frac{Q_{rp}}{h_p}, \forall k \in K, \tag{5}$$

where, $\bar{\upsilon}$ represents the economic speed; l_{rs} represents the distance of voyage leg s on route r; $Q_{rp} = D_{rp}^{+} + D_{rp}^{-}$ represents the sum of the container loading volume D_{rp}^{+} and unloading volume D_{rp}^{-} of port p on route r, and h_p represents the container loading/unloading rate of port p. Therefore, the fixed cost of heterogeneous feeder container fleet C_{oper} is calculated as

$$C_{oper} = C_{oil}^{oper} \sum_{r \in R} \sum_{k \in K_1} \frac{T_{rk}^{sail} + T_{rk}^{hand}}{24} x_{rk} + C_{LNG}^{oper} \sum_{r \in R} \sum_{k \in K_2} \frac{T_{rk}^{sail} + T_{rk}^{hand}}{24} y_{rk}. \tag{6}$$

Table 1. Model parameters and variables

Symbol	Definition
Q_{rp}	The total amount of handling containers at port p on route r (TEUs)
D_{rp}^{+}	The container loading volume of port p on route r (TEUs)
D_{rp}^{-}	The container unloading volume of port p on route r (TEUs)
h_p	The container loading/unloading rate of port p (TEUs/hour)
W_k^{oil}	The maximum capacity in TEUs of an OFS (TEUs)
W_k^{LNG}	The maximum capacity in TEUs of an LFS (TEUs)
l_{rs}	The distance of voyage leg s of route r (nmi)
V_{min}	Minimum fuel volume for the LNG tank of an LFS (mt)
V_{max}	Holding capacity for the LNG tank of an LFS (mt)
FC_k	The fuel consumption rate of an OFS (tons/nmi)
FL_k	The fuel consumption rate of an LFS (tons/nmi)
FR_p	The bunkering speed at port p (mt/hour)
δ_{oil}	The carbon emission factor of LSFO (tonsCO_2/mt)
δ_{LNG}	The carbon emission factor of LNG (tonsCO_2/mt)
$\bar{\upsilon}$	The economic speed (knots)
c_{oper}^{oil}	The unit fixed cost of OFS (USD/day)
c_{oper}^{LNG}	The unit fixed cost of LFS (USD/day)
c_{rpk}^{hand}	The unit container handling cost of ship k at port p of route r (USD/TEU)
f_{e1}	The unit emission cost of LSFO (USD/tons)
f_{e2}	The unit emission cost of LNG (USD/tons)
f_{oil}	The unit cost of LSFO (USD/tons)
f_{LNG}	The unit cost of LNG (USD/tons)
$x_{rk} \in \{0,1\}$	1 if an LFS k serves route r and 0 otherwise
$y_{rk} \in \{0,1\}$	1 if an OFS k serves route r and 0 otherwise
$\varepsilon_{rk(p,p+1)} \in \{0,1\}$	1 If ship k sails from port p to port $p+1$ on route r and 0 otherwise
$z_{rsk} \in \{0,1\}$	1 if an LFS k bunkers at the port of voyage leg s of route r and 0 otherwise

Here, C_{oil}^{oper} and C_{LNG}^{oper} represent the fixed cost of an OFS and LFS, respectively.

3.2.2. The Container Handling Cost

The container handling costs are conventionally decomposed into the cost of unloading and loading containers [34]. Then, this study assumes that the container loading and unloading rates vary across each port. Meanwhile, c_{rpk}^{hand} is the unit container handling cost of ship k at port p on route r. Hence, the container handling cost $C_{handling}$ is given as

$$C_{handling} = \sum_{r\in R}\sum_{p\in P_r}\sum_{k\in K} c_{rpk}^{hand} Q_{rp} x_{rk}. \tag{7}$$

3.2.3. The Fuel Consumption Cost

Generally, the ship speed has a significant impact on the fuel consumption rate of the feeder container ship and shows a power-law relationship, that is, the higher the ship speed, the faster the fuel consumption rate of the ship [14, 35, 36]. Meanwhile, considering the differences in fuel types employed by OFSs and LFSs, this study quantifies the fuel consumption rates of OFSs and LFSs as FC_k and FL_k, respectively, and given as

$$FC_k = \frac{\gamma_k \cdot (\bar{\upsilon})^{(\tau_k - 1)}}{24}, \forall k \in K_1, \tag{8}$$

$$FL_k = \frac{a_k \cdot (\bar{\upsilon})^{(b_k - 1)}}{24}, \forall k \in K_2. \tag{9}$$

Here, γ_k and τ_k are the coefficients of the LSFO consumption rate function; a_k and b_k are the coefficients of the LNG consumption rate function. Hence, the LFSO consumption cost of OFSs C_{fuel1} is obtained as

$$C_{fuel1} = f_{oil}\sum_{r\in R}\sum_{s\in S_r}\sum_{k\in K_1} l_{rs} FC_k, \tag{10}$$

the LNG consumption cost of LFSs C_{fuel2} is obtained as

$$C_{fuel2} = f_{LNG}\sum_{r\in R}\sum_{s\in S_r}\sum_{k\in K_2} l_{rs} FL_k + f_{LNG}\sum_{r\in R}\sum_{s\in S_r}\sum_{k\in K_2} z_{rsk} B_{rs}. \tag{11}$$

Here, f_{oil} is the unit cost of LSFO; f_{LNG} indicates the unit bunker cost of LNG, and B_{rs} indicates the total LNG bunkering volume of ship k at voyage leg s of route r. Therefore, the fuel consumption cost of heterogeneous feeder container fleet is given as

$$\begin{aligned} C_{fuel} &= C_{fuel1} + C_{fuel2} \\ &= f_{oil}\sum_{r\in R}\sum_{s\in S_r}\sum_{k\in K_1} l_{rs} FC_k + f_{LNG}\sum_{r\in R}\sum_{s\in S_r}\sum_{k\in K_2} l_{rs} FL_k \\ &+ f_{LNG}\sum_{r\in R}\sum_{s\in S_r}\sum_{k\in K_2} z_{rsk} B_{rs}. \end{aligned} \tag{12}$$

3.2.4. The Carbon Emission Cost in Sea

During the voyage, the carbon emission cost in sea is not only correlated with fuel consumption volume, but also directly related to the carbon emission factor of the fuel used [12]. To this end, this study defines δ_{oil} and δ_{LNG} as the carbon emission factors of LSFO and LNG, respectively. Notably, the carbon emission factor units for δ_{oil} and δ_{LNG} are tons of CO_2 per mt of fuel, abbreviated as tonsCO_2/mt. Hence, the carbon emission cost in sea of the heterogeneous feeder container fleet C_{emis} is calculated as

$$C_{emis} = f_{e1}\sum_{r\in R}\sum_{s\in S_r}\sum_{k\in K_1} \delta_{oil} l_{rs} FC_k + f_{e2}\sum_{r\in R}\sum_{s\in S_r}\sum_{k\in K_2} \delta_{LNG} l_{rs} FL_k. \tag{13}$$

Here, f_{e1} and f_{e2} indicate the unit emission costs of LSFO and LNG, respectively.

3.2.5. The User Timeliness Satisfaction

In this subsection, this study proposes a user timeliness satisfaction function that integrates prospect theory with fuzzy time windows. This function accurately quantifies users' irrational psychological behavior and the service performance of the heterogeneous feeder container fleet. Next, the fuzzy time window is divided into the expected berthing time window $[ET_p, LT_p]$, acceptable berthing time window $[EAT_p, LAT_p]$, and penalty time window $[0, EAT_p] \cup [LAT_p, +\infty]$. $[ET_p, LT_p]$ as the reference point. In detail, if the ship berths within $[ET_p, LT_p]$, the user timeliness satisfaction is equal to 1. If the ship berths within $[EAT_p, ET_p)$ or $[LT_p, LAT_p)$, the user timeliness satisfaction gradually increases or decreases, respectively. If the ship berths within $[0, EAT_p]$ and $[LAT_p, +\infty)$, the user timeliness satisfaction is equal to 0. Then, the user timeliness satisfaction function is expressed as

$$M_k\left(t_{rp}^{arr}\right) = \begin{cases} 0, & t_{rp}^{arr} < EAT_p; \\ \left(\dfrac{t_{rp}^{arr} - EAT_p}{ET_p - EAT_p}\right)^{\alpha}, & EAT_p \le t_{rp}^{arr} < ET_p; \\ 1, & ET_p \le t_{rp}^{arr} < LT_p; \\ 1 - \lambda\left(\dfrac{t_{rp}^{arr} - LT_p}{LAT_p - LT_p}\right)^{\beta}, & LT_p \le t_{rp}^{arr} < LAT_p; \\ 0, & t_{rp}^{arr} \ge LAT_p. \end{cases} \quad (14)$$

Then, this study adopts the average timeliness satisfaction to express the overall timeliness satisfaction of all users. Accordingly, the average timeliness satisfaction is defined as

$$\bar{M} = \frac{1}{P}\left(\iota_1 \sum_{p\in P_r}\sum_{k\in K_1} M_k\left(t_{rp}^{arr}\right) + \iota_2 \sum_{p\in P_r}\sum_{k\in K_2} M_k\left(t_{rp}^{arr}\right)\right). \quad (15)$$

Here, $\iota_1 \in (0.1)$ and $\iota_2 \in (0.1)$ are defined as the timeliness satisfaction weighting factors for OFSs and LFSs, respectively. The user timeliness satisfaction function is shown in Figure. 3.

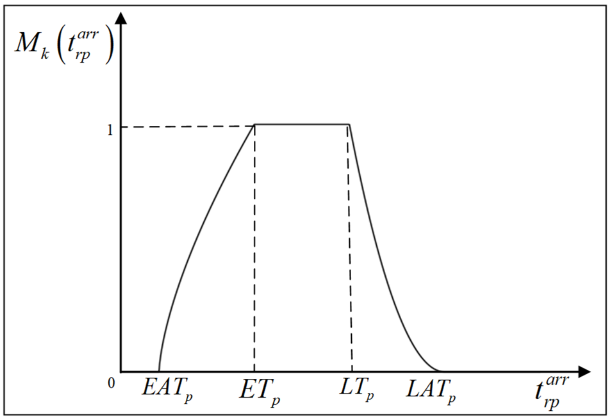

Figure 3. The graph of user timeliness satisfaction

3.2.6. The Mathematical Formula

Based on the above derivation process, the bi-objective mixed-integer nonlinear programming model is obtained as

$$\begin{aligned} \min C &= C_{oper} + C_{handling} + C_{fuel} + C_{emis} \\ &= C_{oil}^{oper} \sum_{r\in R}\sum_{k\in K_1} \frac{T_{rk}^{sail} + T_{rk}^{hand}}{24} \cdot x_{rk} \\ &+ C_{LNG}^{oper} \sum_{r\in R}\sum_{k\in K_2} \frac{T_{rk}^{sail} + T_{rk}^{hand}}{24} \cdot y_{rk} + \sum_{r\in R}\sum_{p\in P_r}\sum_{k\in K} c_{rpk}^{hand} Q_{rp} x_{rk} \\ &+ f_{oil} \sum_{r\in R}\sum_{s\in S_r}\sum_{k\in K_1} l_{rs} FC_k + f_{LNG} \sum_{r\in R}\sum_{s\in S_r}\sum_{k\in K_2} l_{rs} FL_k \\ &+ f_{LNG} \sum_{r\in R}\sum_{s\in S_r}\sum_{k\in K_2} z_{rsk} B_{rs} + f_{e1} \sum_{r\in R}\sum_{s\in S_r}\sum_{k\in K_1} \delta_{oil} l_{rs} FC_k \\ &+ f_{e2} \sum_{r\in R}\sum_{s\in S_r}\sum_{k\in K_2} \delta_{LNG} l_{rs} FL_k, \end{aligned} \quad (16)$$

$$\max \bar{M} = \frac{1}{P}\left(\iota_1 \sum_{r\in R}\sum_{p\in P_r}\sum_{k\in K_1} M_k\left(t_{rp}^{arr}\right) + \iota_2 \sum_{r\in R}\sum_{p\in P_r}\sum_{k\in K_2} M_k\left(t_{rp}^{arr}\right)\right). \quad (17)$$

s.t.

$$\sum_{p\in P_r} \varepsilon_{rk(p,p+1)} = 1, \forall r \in R, k \in K, \quad (18)$$

$$\sum_{p\in P_r} \varepsilon_{rk(0,p)} = \sum_{p\in P_r} \varepsilon_{rk(p,0)} = 1, \forall r \in R, k \in K, \quad (19)$$

$$\sum_{r\in R}\sum_{p\in P_r} \varepsilon_{rk(0,p)} D_{rp}^{+} \le W_k^{oil}, \forall k \in K_1, \quad (20)$$

$$\sum_{r\in R}\sum_{p\in P_r} \varepsilon_{rk(0,p)} D_{rp}^{+} \le W_k^{LNG}, \forall k \in K_2, \quad (21)$$

$$G_{r(p+1)k} = G_{rpk} - \varepsilon_{rk(p,p+1)}\left(D_{r(p+1)}^{-} - D_{r(p+1)}^{+}\right), \forall r \in R, p \in P_r, k \in K, \quad (22)$$

$$G_{r(p+1)k} - \varepsilon_{rk(p,p+1)}\left(D_{r(p+1)}^{-} - D_{r(p+1)}^{+}\right) \le W_k^{oil}, \forall r \in R, p \in P_r, k \in K_1, \quad (23)$$

$$\varepsilon_{rk(p,p+1)}\left(D_{r(p+1)}^{-} - D_{r(p+1)}^{+}\right) + G_{r(p+1)k} \le W_{rpk}^{LNG}, \forall r \in R, p \in P_r, k \in K_2, \quad (24)$$

$$V_{rs} = V_{r(s-1)} + \sum_{r\in R}\sum_{s\in S_r}\sum_{k\in K_2} z_{rsk} B_{rs} - \sum_{r\in R}\sum_{s\in S_r} l_{rs} FL_k, \forall r \in R, s \in S_r, k \in K_2, \quad (25)$$

$$V_{r(s-1)} - \sum_{r\in R}\sum_{s\in S_r} l_{rs} FL_k \ge V_{\min}, \forall r \in R, s \in S_r, k \in K_2, \quad (26)$$

$$V_{r(s-1)} + \sum_{r\in R}\sum_{s\in S_r}\sum_{k\in K_2} z_{rsk} B_{rs} \le V_{\max}, \forall r \in R, s \in S_r, k \in K_2, \quad (27)$$

$$B_{rs} \le V_{\max} - V_{rs}, \forall r \in R, s \in S_r, k \in K_2, \quad (28)$$

$$t_{rp}^{fill} = \frac{V_{\max} - V_{rs}}{FR_p}, \forall r \in R, p \in P_r, s \in S_r, k \in K_2, \quad (29)$$

$$t_{rp}^{hand} = \frac{Q_{rp}}{h_p}, \forall r \in R, p \in P_r, h_p \in H_{rp}, \quad (30)$$

$$t_{rs}^{sail} = \frac{l_{rs}}{\upsilon}, \forall r \in R, s \in S_r, \quad (31)$$

$$t_{r(p+1)}^{wait} \ge ET_p - t_{rp}^{dep} - t_{rp}^{sail}, \forall r \in R, p \in P_r, \quad (32)$$

$$t_{r(p+1)}^{arr} = t_{rp}^{dep} + t_{rs}^{sail}, \forall r \in R, p \in P_r, s \in S_r, \tag{33}$$

$$t_{rp}^{dep} = t_{rp}^{arr} + t_{rp}^{wait} + t_{rp}^{hand}, \forall r \in R, p \in P_r, \tag{34}$$

$$\begin{gathered} \varepsilon_{rk(p,p+1)} \left(t_{rp}^{arr} + t_{rp}^{wait} + t_{rp}^{hand} + t_{rs}^{sail} - t_{r(p+1)}^{arr} \right) = 0, \\ \forall r \in R, p \in P_r, s \in S_r, k \in K, \end{gathered} \tag{35}$$

$$u_{rp} + u_{r(p+1)} + n\varepsilon_{r(p,p+1)} \leq n-1, \forall r \in R, p \in P_r, \tag{36}$$

$$x_{rk} \in \{0,1\}, \forall r \in R, k \in K_1, \tag{37}$$

$$y_{rk} \in \{0,1\}, \forall r \in R, k \in K_2, \tag{38}$$

$$z_{rsk} \in \{0,1\}, \forall r \in R, k \in K_2, s \in S_r, \tag{39}$$

$$\varepsilon_{rk(p,p+1)} \in \{0,1\}, \forall r \in R, k \in K, p \in P_r. \tag{40}$$

Equations (16)-(17) are the bi-objective function. Constraint (18) indicates that each port is only called at once. Constraint (19) ensures that each ship departs from and returns to the hub port. Constraints (20)-(21) limit the ship's load at the hub port departure to its rated load capacity. Constraint (22) is the ship's remaining containers at each port after the handling work. Constraints (23)-(24) indicate that the ship's load is not more than its rated load capacity after the handling work. Constraint (25) calculates the remaining LNG volume of LFSs after completing the voyage leg s in the loaded state. Constraint (26) ensures that the remaining LNG volume of LFS meets the minimum fuel requirements of the LNG tank after completing segment s. Constraints (27)-(28) ensure that the LNG bunkering volume remains within the allowable capacity of the LNG tank. Constraint (29) defines LFS's LNG bunkering time. Constraint (30) specifies the ship's container handling time. Constraint (31) denotes the ship's sailing time on voyage leg s. Constraint (32) describes the ship's waiting time at each port. Constraint (33) indicates the ship's arrival time. Constraint (34) determines the ship's departure time. Constraint (35) ensures the continuity of the ship's sailing time. Constraint (36) imposes the sub-tour elimination constraint for the transportation route. Constraints (37)-(40) specify the values of the associated decision variables.

4. Solution Approach

In this section, considering the complexity of the HFCF-UTS model and the specificity of its application scenarios, this study proposes an ASVNLNS algorithm within the classical ALNS framework. The proposed ASVNLNS innovatively improves the operator scoring mechanism, which significantly enhances search efficiency and the quality of the solutions obtained. Then, Figure. 4 illustrates the ASVNLNS algorithm flow.

4.1. Initial Solution

This study designs a heuristic rule algorithm to generate an initial feasible solution, which enhances the probability of finding the best solution x_{best} and accelerates the subsequent iterative process. Before initialization, the demands of each user are known. Then, based on the constraints of the maximum sailing distance and the maximum loading capacity of the heterogeneous feeder container fleet, this algorithm seeks the closest port from the current port that has unmet demand as the next service object according to the heuristic rule, and ultimately generates a suitable and high-quality initial feasible solution. The specific steps of the heuristic rule algorithm are shown in Table 2.

4.2. Removal Operators

In this subsection, this study mainly introduces three removal operators, including random removal, Shaw removal, and worst removal. In each iterative process, the removal operator selects and removes $q = \mu \cdot N$ ports from the current solution x_s, and temporarily stores these removed ports in the set TS. Among them, μ represents the degree of removal. N represents the total number of ports of x_s.

4.2.1. Random Removal

The random removal randomly removes q ports from x_s, and temporarily stores these ports in TS.

4.2.2. Shaw Removal

The Shaw removal is adopted to compute the similarity between ports i and j by utilizing the relatedness function $\Gamma(i,j)$, storing these similarities in TL. Among them, the distance between ports and the container unloading volume of each port as key attributes to quantify this similarity [22, 37]. The specific calculation formula is expressed as

$$\Gamma(i,j) = \phi d_{ij} + \kappa \left| D_{ri}^{+} - D_{rj}^{+} \right|, \tag{41}$$

where, d_{ij} is the distance between port i and j; ϕ and κ represent the weight coefficient. Based on the above steps, sort these similarities in TL in ascending order, remove the port with highest relatedness, and insert it in TS. Finally, repeat the above steps q times, and obtain the broken solution x_s^* and the set TS of ports to be reinserted.

4.2.3. Worst Removal

The worst removal measures the cost difference that each port is removed from the current position in x_s, aiming to remove the high-cost request. For this purpose, this study defines the DIF to represent the differences brought by each port [42]. The specific calculation formula is obtained as

$$DIF = \frac{C(x_s) - C_{-i}(x_s)}{\left(\bar{M}(x_s) - \bar{M}_{-i}(x_s) \right) \cdot 100}. \tag{42}$$

Here, $C(x_s)$ and $\bar{M}(x_s)$ represent the total turnaround cost and user timeliness satisfaction of x_s, respectively; $C_{-i}(x_s)$ and $\bar{M}_{-i}(x_s)$ represent the total turnaround cost and user timeliness satisfaction after assuming the removal of port i in x_s. Next, all DIF are collected into TL, sorted in ascending order, and randomly selected from its. The selected DIF is then put into TS for the subsequent insertion operator. This operator does not terminate until q ports have been inserted into TS , only then is the x_s^* obtained.

4.3. Insertion Operators

This study employs three insertion operators, including random insertion, regret insertion, and best insertion, to repair x_s^* and generate a new solution x_{new}. Specifically, the operator reinserts the q removed ports of TS into x_s^*

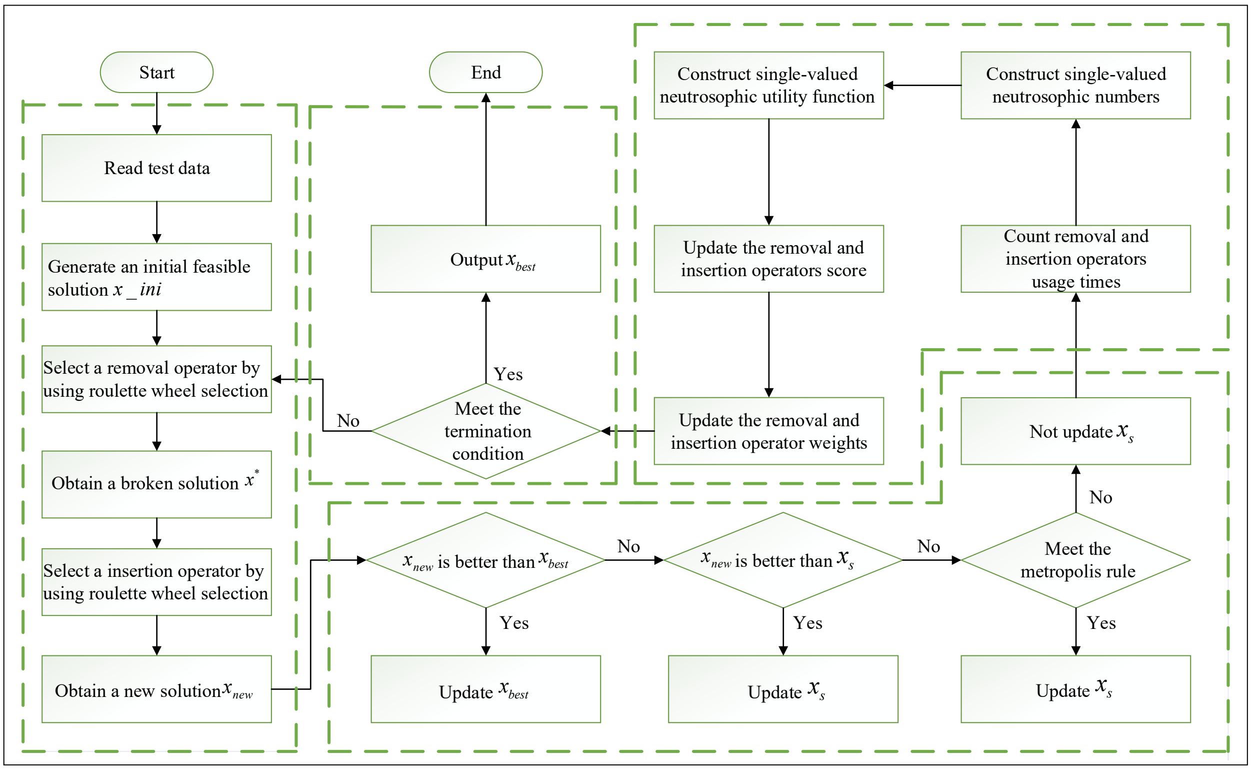

Figure 4. The ASVNLNS algorithm flow chart

according to the certain criteria. The insertion work stops until the TS is an empty set, and finally obtain the x_{new}.

4.3.1. Random Insertion

This operator randomly selects a removed port i from TS, and randomly reinserts it into x_s^*. Then, the OFS routes only need to meet the ship's load capacity constraints, while LFS routes additionally meet the ship's load capacity constraints and also follow the maximum sailing distance constraints. Repeat the above steps until all ports in TS are reinserted and then stop, and finally generate x_{new}.

4.3.2. Regret Insertion

This operator inserts the removed request into the best insertion position, which reduces the insertion cost and maximizes the benefit [22, 38]. For this purpose, this study defines ψ_1 and ψ_2 as the measures of user timeliness satisfaction corresponding to inserting the removed port i into the best insertion position j_1 and secondly insertion position j_2 of x_s^*, respectively. Then, store the regret values $\Delta_{RC} = \psi_1 - \psi_2$ of the port i in the set RV and sort them in descending order. Next, select the high regret value for port i and insert it into x_s^*.

4.3.3. Best Insertion

Under the constraint of solution feasibility, the best insertion operator computes the insertion costs incurred by the removed port i at all possible positions of x_s^* and stores these in the set BV. This operator then sorts these insertion costs of port i in BV in descending order, and selects the position with the minimum insertion cost. This operator stops only after all ports in TS have been inserted into x_s^*.

4.4. Adaptive Strategy

4.4.1. Roulette Wheel Mechanism

The roulette wheel mechanism is employed to choose the removal and insertion operators. Among them, each operator is equipped with a weight $\omega_i (i = 1,2,3, \ldots, n)$, which reflects its historical performance. Therefore, the probability that operator j is randomly selected is $\varphi = \omega_j / \sum_{i=1}^{n} \omega_i$, and the weight of each operator is set to 1 during the first iteration.

4.4.2. Operator Weight Adaptive Update

This study divides the running process of ASVNLNS into 5 segments, and each segment consists of 100 iterations. Before the ASVNLNS algorithm starts, the initial weight and score of each operator are set to 1 and 0, respectively. During the run of each segment, this study employs the θ_1, θ_2, θ_3, and θ_4 to count the number of uses for each operator in the four scoring situations of segment seg, respectively. Depending on the quality of x_{new}, the ASVNLNS algorithm assigns scores ϑ_1, ϑ_2, ϑ_3, and ϑ_4 for each operator in the four scoring situations, and meets $\vartheta_1 > \vartheta_2 > \vartheta_3 > \vartheta_4$. Then, the four scoring situations are as follows.

If the bi-objective function value of x_{new} is better than x_{best}, update x_{best} to x_{new}, assign score ϑ_1 for the utilized operator, and θ_1 plus 1, it gets

$$C(x_{new}) \geq C(x_{best}), and\ \bar{M}(x_{new}) \leq \bar{M}(x_{best}). \tag{43}$$

Otherwise, if the bi-objective function value of x_{new} is worse than x_{best} and better than x_s, update x_{best} to x_s, assign score ϑ_2 for the utilized operator, and θ_2 plus 1, it gets

$$C(x_{new}) \geq C(x_s), and\ \bar{M}(x_{new}) \leq \bar{M}(x_s). \tag{44}$$

Otherwise, if the bi-objective function value of x_{new} in at least one is better than x_s, accept x_{new} according to a certain probability, assign score ϑ_3 for the utilized operator, and θ_3 plus 1, it gets

$$C(x_{new}) \geq C(x_s), or\ \bar{M}(x_{new}) \leq \bar{M}(x_s). \tag{45}$$

Otherwise, x_{new} is not accepted, assign score ϑ_4 for the utilized operator, and θ_4 plus 1. Then, a truth-membership degree T_N, an indeterminacy-membership degree I_N, and a falsity-membership degree F_N of single-valued neutrosophic number $N = \langle T_N, I_N, F_N \rangle$ are respectively obtained as

$$T_N = \frac{\partial \theta_1}{\sum_{i=1}^{4} \theta_i}, I_N = \frac{\theta_2}{\sum_{i=1}^{4} \theta_i}, F_N = \frac{\theta_3 + \theta_4}{\sum_{i=1}^{4} \theta_i}, \quad (46)$$

Table 2. The pseudocode of heuristic rule

	Algorithm 1: Heuristic rule.
1	**Input:** a set of ports N, a set of distances between each port Dis, the maximum sailing distance of LFS max_LNG_dis, the maximum capacity in TEUs of LFS and OFS W_k^{LNG} and W_k^{oil}, respectively;
2	create an empty set of initial feasible solutions x_{ini};
3	create an empty Boolean set Bol, and set the status of hub port and each port to True and False, respectively;
4	create an empty set of current routes $x_{current}$ and set the hub port as the start point.
5	**Repeat**
6	Find a closest unserved port i with the hub port and insert it into $x_{current}$;
7	Set the status of visited port i in Bol to True;
8	**If** the total sailing distance of $x_{current}$ is not less than max_LNG_dis **then**
9	Set the $x_{current}$ as a route of LFS;
10	**If** the total loading capacity of $x_{current}$ is not less than W_k^{LNG} **then**
11	Expand from port i to the nearest port j and update $x_{current}$;
12	Set the status of visited port j in Bol to True;
13	**Else**
14	Append the hub port to $x_{current}$, put $x_{current}$ into x_{ini}, and set $x_{current}$ empty again;
15	Return step 6;
16	**If** the total sailing distance of $x_{current}$ is less than max_LNG_dis **then**
17	Expand from port i to the nearest bunker port j and update $x_{current}$;
18	Set the status of visited port j in Bol to True;
19	**Else**
20	Set the $x_{current}$ as a route of OFS;
21	**If** the total loading capacity of $x_{current}$ is not less than W_k^{oil} **then**
22	Expand from port i to the nearest port j and update $x_{current}$;
23	Set the status of visited port j in Bol to True;
24	**Else**
25	Append the hub port to $x_{current}$, put $x_{current}$ into x_{ini}, and set $x_{current}$ empty again;
26	Return step 6;
27	**Until** all ports are served, and the status of all ports in Bol is True;
28	**Output:** initial feasible solution x_{ini}.

where, $\partial \in (0, 1)$ is a correction factor. Hence, the single-valued neutrosophic utility function is formed as

$$u = \frac{1-g}{\varphi g}\left(\frac{\varphi\left(T_N + F_N\right)\left(T_N - F_N + 1\right)}{2\left(1-g\right)} + o\right)^g, \quad (47)$$

where, g, φ, and o are the parameters of this function [39]. Therefore, the new weight $\omega_{i,seg+1}$ and new score σ_i^* of operator i are expressed as

$$\sigma_i^* = \begin{cases} u\left(\vartheta_c - \vartheta_{c+1}\right) + \vartheta_{c+1}, & c \in [1,3]; \\ u\vartheta_c, & c = 4, \end{cases} \quad (48)$$

$$\omega_{i,seg+1} = \begin{cases} \omega_{i,seg}\left(1-\varsigma\right) + \varsigma \dfrac{\sigma_i^*}{\theta_i}, \theta_i \neq 0; \\ \omega_{i,seg}, \theta_i = 0, \end{cases} \quad (49)$$

where, $\varsigma \in (0, 1)$ is the reaction factor.

4.5. Acceptance and Stopping Criteria

Based on the description in subsection 4.4, if x_{new} is better than x_s, then the strategy of replacing x_s with x_{new} is adopted. Otherwise, the ASVNLNS algorithm follows the acceptance criterion of simulated annealing and accepts x_{new} with a certain probability $e^{-(x_{new}-x_s)/T}$. In detail, this study establishes T as the current temperature and initializes it as $T = T_0$. Meanwhile, the initial temperature T_0 is set as $-\xi \cdot |x_s|/ln\varrho$, make sure that x_{new} is ξ% worse than x_s, there is still a ϱ% probability of being accepted. Then, this standard gradually reduces the possibility of accepting poor solutions by setting $T = T \cdot \chi$ to lower the temperature. Among them, $\chi \in (0,1)$ represents the cooling rate. Notably, the $x_{new} - x_s$ is equivalent to the sum of the differences between the total turnaround cost corresponding to x_{new} and x_s and the customer's timeliness satisfaction.

5. Results

For convenience, the instance description and parameter setting are introduced in subsection 5.1. The optimization results of the ASVNLNS algorithm are introduced in subsection 5.2. The comparative analysis between ALNS and ASVNLNS is presented in subsection 5.3. The sensitive analysis is introduced in subsection 5.4.

5.1. Study Case

A test instance set was established using instances A1, A2, B2, B3, C2, and C3 in reference [9], derived from the real operational data of a Norwegian shipping line. Among them, instances A1 and A2 are small-scale instances, each containing 10 ports. Instances B2 and B3 are medium-scale instances, each containing 15 ports. Instances C2 and C3 are large-scale instances, each containing 22 ports. Particularly, the hub port for each instance is the Rotterdam port. Then, based on reviewing references and interviewing experienced captains, the container handling volume at each port for all instances was appropriately adjusted and randomly assigned to the corresponding time window. Second, the ports of Gjemnes and Salten were replaced with Vestbase and Bodø, respectively, and the ports of Bergen, Ålesund, Sunndalsøra, and Høyanger were designated as LNG bunkering ports, according to the distribution of Norwegian LNG bunkering ports on the SEA-LNG website. This website is https://sea-lng.org/bunker-navigator/.

For convenience, the data of the test instance set are detailed in Tables 3-8. In Tables 3-8, "PN", "UV", and "LV" represent the port name, unloading volume of a port, and loading volume of a port, respectively. "ET" and "AT" represent the expected and acceptable berthing time windows for a ship, respectively. Additionally, the port distribution is shown in Figure. 5. The parameter values used in the HFCF-UTS model and ASVNLNS algorithm are detailed in Tables 9 and 10 [12, 14, 22, 37, 40].

Table 3. The feeder port information of instance A1

PN	UV	LV	ET	AT
Håvik	150	250	9:07-1:07	8:07-3:07
Haugesund	80	102	19:33-13:33	17:33-14:33
Husnes	700	180	21:39-23:39	20:39-1:39
Svelgen	320	310	6:14-1:14	5:14-3:14
Ikornnes	50	40	6:07-7:07	4:07-9:07
Ålesund	199	166	18:58-19:58	16:58-20:58
Molde	110	100	4:48-21:48	2:48-22:48
Vestbase	500	500	18:03-14:03	17:03-15:03
Orkanger	560	470	5:34-4:34	3:34-5:34

Table 4. The feeder port information of instance A2

PN	UV	LV	ET	AT
Tananger	95	123	22:53-23:53	20:53-1:53
Haugesund	80	102	22:18-20:18	21:18-22:18
Bergen	79	143	0:55-16:55	22:55-17:55
Florø	370	370	23:20-3:20	22:20-5:20
Måløy	370	830	11:47-5:47	9:47-6:47
Ålesund	199	166	4:27-2:27	3:27-4:27
Molde	110	100	17:09-11:09	15:09-13:09
Vestbase	500	500	8:00-8:00	6:00-10:00
Orkanger	560	470	8:41-1:41	6:41-2:41

Table 5. The feeder port information of instance B2

PN	UV	LV	ET	AT
Egersund	650	200	16:42-8:42	14:42-9:42
Haugesund	80	102	3:46-7:46	2:46-9:46
Bergen	79	143	2:08-1:08	1:08-3:08
Høyanger	200	150	16:56-15:56	14:56-17:56
Måløy	370	830	10:31-4:31	8:31-5:31
Hareid	600	700	22:47-2:47	21:47-3:47
Ikornnes	50	40	5:40-23:40	3:40-0:40
Molde	110	100	16:31-20:31	14:31-22:31
Sunndalsøra	200	370	22:56-2:56	20:56-4:56
Vestbase	500	500	11:29-6:29	9:29-7:29
Averøy	260	170	9:50-5:50	8:50-6:50
Glomfjord	170	170	5:00-22:00	3:00-23:00
Bodø	690	490	23:13-16:13	22:13-18:13
Stokmarknes	100	260	8:12-2:12	6:12-3:12

Table 6. The feeder port information of instance B3

PN	UV	LV	ET	AT
Egersund	650	200	10:39-2:39	9:39-3:39
Håvik	150	250	0:56-17:56	22:56-18:56
Husnes	700	180	7:05-0:05	5:05-2:05
Bergen	79	143	7:21-0:21	6:21-2:21
Høyanger	200	150	12:50-6:50	11:50-7:50
Florø	370	370	14:55-6:55	13:55-7:55
Svelgen	320	310	13:11-6:11	11:11-8:11
Måløy	370	830	10:01-3:01	8:01-5:01
Sunndalsøra	200	370	16:56-10:56	15:56-11:56
Vestbase	500	500	5:44-21:44	4:44-22:44
Averøy	260	170	15:24-7:24	14:24-8:24
Orkanger	560	470	1:04-17:04	0:04-19:04
Glomfjord	170	170	1:47-18:47	23:47-20:47
Bodø	690	490	11:03-3:03	10:03-4:03

Table 7. The feeder port information of instance C2

PN	UV	LV	ET	AT
Egersund	650	200	0:11-1:11[+1]	22:11-2:11
Tananger	95	123	21:47-19:47	20:47-21:47
Håvik	150	250	11:53-6:53	9:53-8:53
Haugesund	80	102	22:30-2:30	21:30-3:30
Husnes	700	180	17:54-11:54	16:54-13:54
Bergen	79	143	5:04-4:04	4:04-5:04
Høyanger	200	150	17:40-12:40	16:40-14:40
Florø	370	370	22:37-18:37	21:37-20:37
Svelgen	320	310	22:23-14:23	21:23-16:23
Måløy	370	830	0:36-21:36	22:36-23:36
Hareid	600	700	10:24-9:24	9:24-10:24
Ikornnes	500	400	5:35-8:35	4:35-9:35
Ålesund	199	166	7:21-10:21	5:21-12:21
Molde	110	100	17:36-14:36	15:36-16:36
Sunndalsøra	200	370	2:50-21:50	0:50-23:50
Vestbase	500	500	16:26-11:26	14:26-12:26
Averøy	260	170	21:30-13:30	19:30-15:30
Orkanger	560	470	16:33-16:33	15:33-18:33
Glomfjord	170	170	11:40-6:40	10:40-8:40
Bodø	690	490	21:15-18:15	20:15-19:15
Stokmarknes	100	260	18:48-19:48	16:48-21:48

Table 8. The feeder port information of instance C3

PN	UV	LV	ET	AT
Egersund	770	220	0:11-1:11	22:11-2:11
Tananger	120	130	21:47-19:47	20:47-21:47
Håvik	210	270	11:53-6:53	9:53-8:53
Haugesund	120	112	22:30-2:30	21:30-3:30
Husnes	940	260	17:54-11:54	16:54-13:54
Bergen	95	227	5:04-4:04	4:04-5:04
Høyanger	280	200	17:40-12:40	16:40-14:40
Florø	380	510	22:37-18:37	21:37-20:37
Svelgen	440	440	22:23-14:23	21:23-16:23
Måløy	58	102	0:36-21:36	22:36-23:36
Hareid	700	810	10:24-9:24	9:24-10:24
Ikornnes	500	600	5:35-8:35	4:35-9:35
Ålesund	282	224	7:21-10:21	5:21-12:21
Molde	154	141	17:36-14:36	15:36-16:36
Sunndalsøra	200	560	2:50-21:50	0:50-23:50
Vestbase	600	700	16:26-11:26	14:26-12:26
Averøy	340	240	21:30-13:30	19:30-15:30
Orkanger	580	580	16:33-16:33	15:33-18:33
Glomfjord	240	210	11:40-6:40	10:40-8:40
Bodø	106	53	21:15-18:15	20:15-19:15
Stokmarknes	130	280	18:48-19:48	16:48-21:48

5.2. Optimization Results

In this subsection, this study applies a computer equipped with an Intel Core i7-14650HX 2.2 GHz and running Windows 11, together with PyCharm 2021 software to implement the ASVNLNS algorithm and address the HFCF-UTS model. Then, the routes and ship allocation plan of each instance obtained by using the ASVNLNS algorithm is expressed in Table 11. The convergence curve of optimal value of the total turnaround cost and user timeliness satisfaction for each instance is shown in Figures. 6-8. Meanwhile, Figure. 9 vividly illustrates the actual scheduling situation of the heterogeneous feeder container fleet, using instance A1 as an example.

It is observed from Figures. 6–8 that the ASVNLNS algorithm exhibited rapid convergence within the first 200 iterations. Specifically, the total turnaround cost is reduced by 164367.80, 99797.47, 24938.90, 173284.83, 310411.98, and 62833.50 across the six selected instances, while the corresponding improvements in user timeliness satisfaction reach 0.089, 0.075, 0.067, 0.056, 0.032, and 0.220. Subsequently, the objective function convergence curves gradually plateaued during the 200–500 iteration interval. Notably, the convergence trajectories for total turnaround cost and user timeliness satisfaction demonstrate near-symmetrical patterns across different instances. Table 11 and

Figure. 9 further reveal that, except for a few routes, LFS achieves a port coverage ratio exceeding 50% across all routes. Moreover, the service scope of OFS is primarily concentrated on ports along the southern Norwegian west coast, whereas LFS extends more extensively to distant western ports.

Figure 5. The graph of port distribution

Table 9. The parameter values of HFCF-UTS model

Parameters	Description	Value
$\bar{v}$	The economic speed (knots)	18.5
γ_k, τ_k	The coefficients of the LSFO consumption rate function	0.012, 3.0
a_k, b_k	The coefficients of the LNG consumption rate function	0.0139, 3.1284
ι_1, ι_2	The timeliness satisfaction weighting factors	0.5, 0.5
FR_p	The bunkering speed at port p (mt/hour)	1000
V_{max}	Holding capacity for the LNG tank of an LFS (mt)	298
V_{min}	Minimum fuel volume for the LNG tank of an LFS (mt)	29.8
f_{oil}	The unit cost of LSFO (USD/tons)	700
f_{LNG}	The unit cost of LNG (USD/tons)	650
f_{e1}	The unit emission cost of LSFO (USD/tons)	32
f_{e2}	The unit emission cost of LNG (USD/tons)	20
δ_{oil}	The carbon emission factor of LSFO (tonsCO_2/mt)	3.144
δ_{LNG}	The carbon emission factor of LNG (tonsCO_2/mt)	2.750
C_{oil}^{oper}	The unit fixed cost of OFS (USD/day)	8000
C_{LNG}^{oper}	The unit fixed cost of LFS (USD/day)	7500
W_k^{oil}, W_k^{LNG}	The maximum capacity in TEUs of an OFS and LFS (TEUs)	1400
c_{rpk}^{hand}	The unit container handling cost of ship k at port p of route r (USD/TEU)	$U[200; 500]$
h_p	The container loading/unloading rate of port p (TEUs/hour)	$U[50; 100]$

Notes: U is a uniformly distributed pseudo-random number within the specified bounds.

Table 10. The parameter values of ASVNLNS algorithm

Symbol	Description	Numerical value
/	The maximum number of iterations	500
μ	The degree of removal	0.6
ϕ, κ	The weight coefficient of the relatedness function	0.75, 0.1
$\vartheta_1, \vartheta_2, \vartheta_3, \vartheta_4$	Operators' score	33, 13, 9, 4
g, φ, o	The parameters of the single-valued neutrosophic utility function	0.5, 0.5, 2
ς	Reaction factor	0.5
∂	Correction factor	0.5
ξ	The initial temperature control parameter	0.07
ϱ	Acceptable probability	0.5
χ	Cooling rate	0.99975

The above analysis demonstrates that the ASVNLNS algorithm successfully balances the bi-objective functions while mitigating the risk of local optima entrapment. Additionally, it validates that the HFCF-UTS model generates high-quality ship scheduling solutions that integrate cost and timeliness satisfaction in real-world applications. Hence, it is suitable for ship distribution scenarios that prioritize user timeliness experience, thereby aligning with the central theme of this study.

Table 11. Six instances of ship transport routes

Instance	Type	Shipping Routes
A1	OFS	Rotterdam→Orkanger→Ikornnes→Håvik→Haugesund→Husnes→Rotterdam
	LFS	Rotterdam→Svelgen→Vestbase→Molde→Ålesund→Rotterdam
A2	OFS	Rotterdam→Haugesund→Rotterdam
	LFS	Rotterdam→Tananger→Måløy→Vestbase→Florø→Molde→Ålesund→Orkanger→Bergen→Rotterdam
B2	OFS	Rotterdam→Egersund→Molde→Haugesund→Glomfjord→Sunndalsøra→Rotterdam Rotterdam→Ikornnes→Hareid→Vestbase→Måløy→Averøy→Stokmarknes→Bodø→Høyanger→Bergen→Rotterdam
	LFS	\
B3	OFS	Rotterdam→Glomfjord→Måløy→Vestbase→Averøy→Bodø→Egersund→Håvik→Orkanger→Husnes→Rotterdam
	LFS	Rotterdam→Sunndalsøra→Høyanger→Florø→Bergen→Svelgen→Rotterdam
C2	OFS	Rotterdam→Bodø→Glomfjord→Tananger→Orkanger→Stokmarknes→Sunndalsøra→Rotterdam
	LFS	Rotterdam→Egersund→Rotterdam Rotterdam→Hareid→Høyanger→Håvik→Florø→Bergen→Molde→Averøy→Ikornnes→Ålesund→Haugesund→Vestbase→Måløy→Svelgen→Husnes→Rotterdam
C3	OFS	Rotterdam→Husnes→Rotterdam Rotterdam→Orkanger→Egersund→Ikornnes→Rotterdam Rotterdam→Tananger→Florø→Haugesund→Bodø→Molde→Svelgen→Måløy→Vestbase→Høyanger→Glomfjord→Ålesund→Håvik→Rotterdam
	LFS	Rotterdam→Sunndalsøra→Bergen→Hareid→Averøy→Stokmarknes→Rotterdam

5.3. Algorithm Comparison Results

To assess the validity of the ASVNLNS algorithm, a comparative experiment was conducted between the proposed ASVNLNS and the ALNS algorithm under the same parameter settings, based on the above test instance set. Then, the ASVNLNS and ALNS algorithms are independently run 10 times, which ensures the reliability and stability of experimental results. Otherwise, this study establishes that the user timeliness satisfaction is first and the total turnaround cost is second as the selection criterion of the optimal solution through reference [41]. Then, Table 12 presents the comparative results of the ASVNLNS and ALNS algorithms in the test instance set, respectively. In Table 12, "C_{opt}" and

"C_{ave}" represent the best and average solution of total turnaround cost, respectively. "$\bar{M}_{opt}$" and "$\bar{M}_{ave}$" represent the best and average solution of user timeliness satisfaction, respectively. "RT" represents the average running time. Meanwhile, $\Delta_{TAC} = \frac{C(ALNS)-C(IALNS)}{C(IALNS)} \times 100\%$ and $\Delta_{SF} = \frac{\bar{M}(IALNS)-\bar{M}(ALNS)}{\bar{M}(ALNS)} \times 100\%$ represent the percentage differences in C_{opt} and $\bar{M}_{opt}$ between the ASVNLNS and ALNS algorithms.

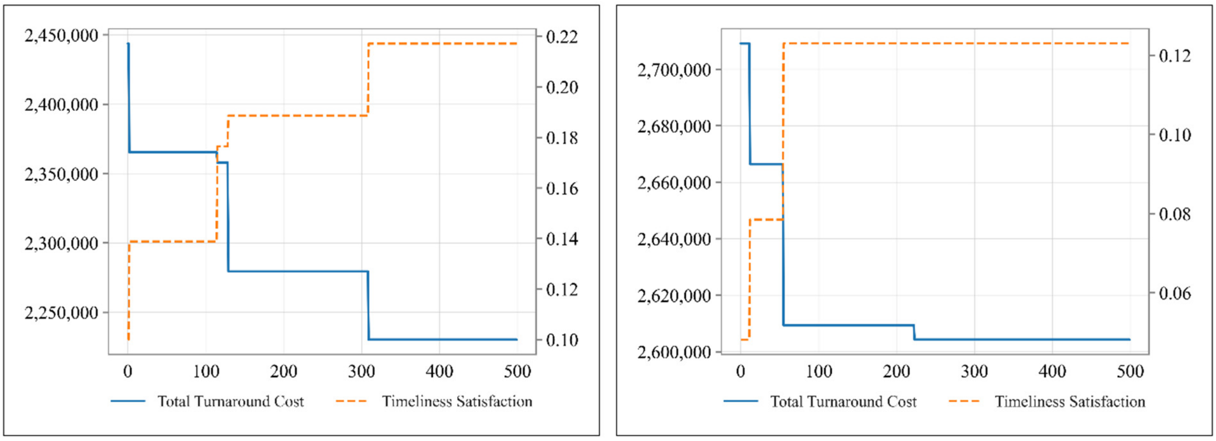

(a) **(b)**

Figure 6. (a) The iterative process of instance A1; **(b)** The iterative process of instance A2

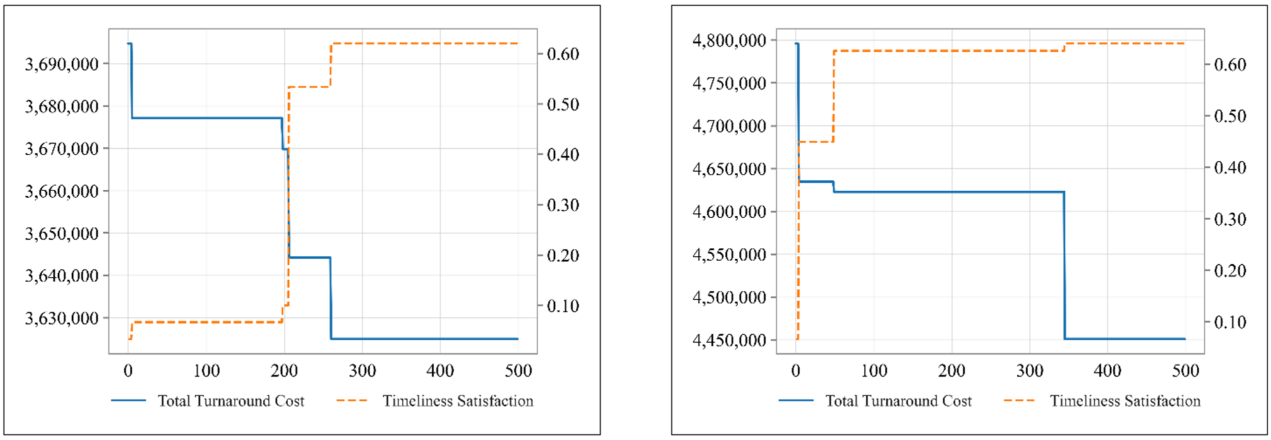

(a) **(b)**

Figure 7. (a) The iterative process of instance B2; **(b)** The iterative process of instance B3

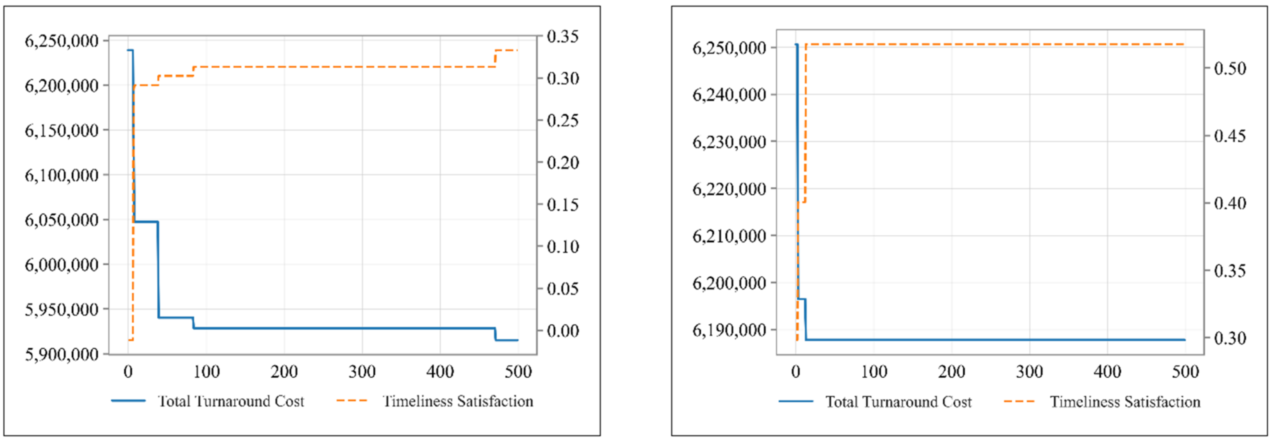

(a) **(b)**

Figure 8. (a) The iterative process of instance C2; **(b)** The iterative process of instance C3

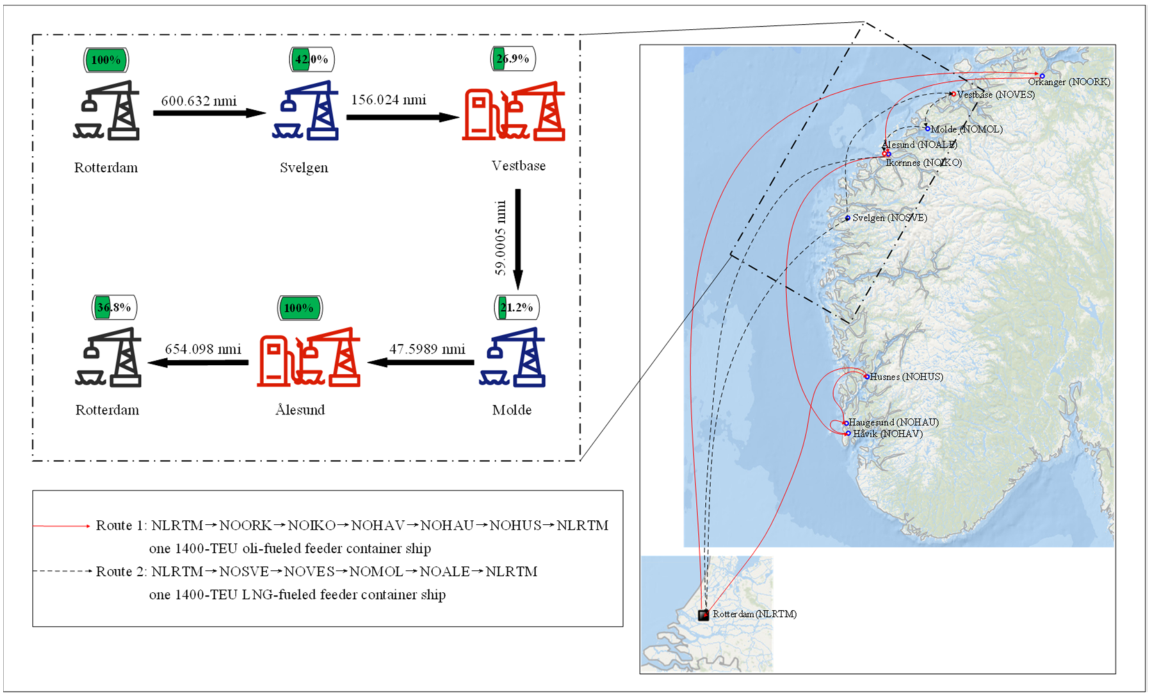

Figure 9. The solution representation of instance A1

It is observed from Table 12 that the number of best solutions obtained is as high as 5 (83.3%) using the ASVNLNS algorithm in the six selected instances. However, the ALNS algorithm has low processing efficiency and only achieves one best solution (16.7%) under the same conditions. Table 12 also represents that the "RT" of the ASVNLNS algorithm is 2.916 seconds slower than the ALNS algorithm, with the fastest reaching 10.021 seconds and the slowest 0.778 seconds. Meanwhile, it is found that the ASVNLNS algorithm possesses an obvious advantage in improving the quality of solution by combining the results of Δ_{TAC} and Δ_{SF}. Notably, the improvement of timeliness satisfaction ranged from 10% to 30%. Furthermore, although the improvement degree of the ASVNLNS algorithm in total turnaround cost is slightly worse than the ALNS algorithm, the difference between the two algorithms is controlled within 5%. Therefore, the performance of the ASVNLNS in achieving a multi-objective balance between timeliness satisfaction and total turnaround cost is more stable and efficient, and shows significant potential in delivery timeliness.

Table 12. Comparison results between the ASVNLNS and ALNS algorithms

Instance	Version	C_{opt}	$\bar{M}_{opt}$	C_{ave}	$\bar{M}_{ave}$	$RT(s)$	$\Delta_{TAC}(\%)$	$\Delta_{SF}(\%)$
A1	ASVNLNS	2230231.202	0.217	2197428.509	0.163	5.721	0.55%	-12.50%
	ALNS	2242460.03	0.248	2170650.084	0.145	6.534		
A2	ASVNLNS	2604293.532	0.123	2508463.107	0.096	6.798	-4.41%	25.51%
	ALNS	2489506.419	0.098	2484486.825	0.083	6.955		
B2	ASVNLNS	3624971.564	0.620	3610504.779	0.428	20.606	-2.35%	13.97%
	ALNS	3539884.006	0.544	3623130.864	0.194	19.828		
B3	ASVNLNS	4451038.196	0.640	4387338.157	0.583	16.214	-3.41%	2.24%
	ALNS	4299178.994	0.626	4436407.185	0.583	17.028		
C2	ASVNLNS	5915111.703	0.333	5768611.100	0.286	47.867	-0.34%	9.18%
	ALNS	5894955.100	0.305	5731358.727	0.267	57.888		
C3	ASVNLNS	6187788.208	0.518	5914028.414	0.486	48.529	-4.72%	9.75%
	ALNS	5895677.993	0.472	5801377.038	0.441	54.998		

5.4. Sensitivity Analysis

To evaluate the influence of the removal degree μ on the performance of the ASVNLNS algorithm, a sensitivity analysis was carried out using instance B3. With all other parameters held constant, the μ was varied from 0.3 to 0.7 in increments of 0.1. For each μ value, the algorithm was randomly run 10 times, and the total turnaround cost and timeliness satisfaction were recorded. The results are presented in Table 13 and Figure.10.

Table 13 and Figure. 10 conclude that as the μ increases, the total turnaround cost and user timeliness satisfaction show a trend of first rising and then falling. Specifically, when the μ is between 0.3 and 0.5, the total turnaround cost shows a slight increase of 2.08%, the user timeliness satisfaction remains stable, and the proportion of LFS in the fleet increases from 0% to 33%. Then, when μ is 0.6, the improvement in user timeliness satisfaction is 2.24%, and the total turnaround cost also decreases accordingly from 4451880.614 to 4451038.196. The proportion of LFS in the fleet has increased from 33% to 50%. It indicates that a stronger μ reduces the operator's reliance on the original feasible solutions, enabling a reduction in fleet size, an increase in the LFS ratio, and a significant improvement in timeliness without significantly increasing costs. Subsequently, when the μ is 0.7, user timeliness satisfaction falls back, while total turnaround cost slightly decreases. Correspondingly, the proportion of LFS in the fleet has dropped from 50% to 33%. It shows that excessive perturbation of the removal operator will disrupt the existing optimal solution structure, increase the search and computational costs of the ASVNLNS algorithm, and thereby lead to a decrease in the quality of the solution. Overall, the analysis of the above results reveals the robustness and stability of the ASVNLNS algorithm, particularly the significant performance of the user timeliness satisfaction function. Additionally, the removal degree significantly affects the total turnaround cost, user satisfaction, and fleet composition of the heterogeneous feeder container fleet, and exhibits obvious non-monotonic characteristics.

Table 13. The operation results under different removal degrees

μ	C_{opt}	$\bar{M}_{opt}$	Fleet Composition	Proportion of LFS	$RT(s)$
0.3	4361158.771	0.626	OFS, OFS, OFS	0%	8.085
0.4	4450991.810	0.626	OFS, OFS, LFS	33%	11.014
0.5	4451880.614	0.626	OFS, OFS, LFS	33%	13.220
0.6	4451038.196	0.640	OFS, LFS	50%	16.214
0.7	4421140.301	0.626	OFS, OFS, LFS	33%	13.518

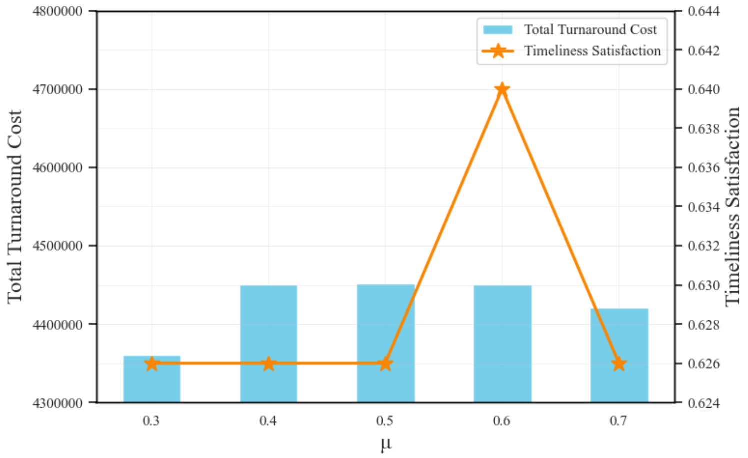

Figure 10. The function values under different removal degrees

6. Conclusion

Based on the above description, this study proposes an HFCF-UTS model and the ASVNLNS algorithm to solve the heterogeneous feeder container ship scheduling problem. The main contributions are as follows.

First, this study proposes the heterogeneous feeder ship fleet operation strategy composed of OFSs and LFSs. This proposed strategy not only promotes the utilization ratio of LFSs but also contributes to improving transportation efficiency and reducing greenhouse gas emissions.

Second, this study develops the HFCF-UTS model to balance total turnaround cost and user timeliness satisfaction functions. Moreover, in the user time-satisfaction function, prospect theory and fuzzy time windows are incorporated to characterize users' tolerance toward delayed deliveries under bounded irrationality.

Third, this study designs an ASVNLNS algorithm, which introduces SvNSs to count the number of used operators and integrates the utility function to accurately evaluate the contribution of each operator and prevent idealized scoring.

The achievements of this study have enriched the literature in the field of heterogeneous feeder container fleet scheduling optimization and provided management insights for decision-makers in shipping enterprises. In addition, to enhance the suitability of the HFCF-UTS model in practical application scenarios, this study will further integrate weather and sea surface data, deepen the analysis of the impact of user psychological behaviors on the scheduling of heterogeneous feeder container fleet, and utilize advanced tools such as reinforcement learning or decision trees to achieve dynamic and effective ship scheduling.

References

[1] United Nations Conference on Trade and Development (UNCTAD), *Review of Maritime Transport 2024*, Geneva: UNCTAD, 2024. [Online]. Available: https://unctad.org/ system/ files/official-document/rmt2024_en.pdf.

[2] D. H. Lee and J. G. Jin, "Feeder vessel management at container transshipment terminals," Transp. Res. Part E: Logist. Transp. Rev., vol. 49, pp. 201–216, Jan. 2013.

[3] S. Jia, C. L. Li, and Z. Xu, "A simulation optimization method for deep-sea vessel berth planning and feeder arrival scheduling at a container port," Transp. Res. Part B: Methodol., vol. 142, pp. 174–196, Dec. 2020.

[4] J. Xu, J. Chen, J. Li, et al., "Transitioning to clean energy in global shipping: Country-based differences and industrial chain collaboration," Ocean Coast Manage., vol. 269, pp. 107752, Oct. 2025.

[5] P. Korlak, E. Złoczowska, and C. Behrendt, "Utilization of waste heat and cold on the example of an LNG-fueled ultra-large container ship," Energy Rep., vol. 12, pp. 3488–3503, Dec. 2024.

[6] X. Chen, R. Hu, K. Luo, et al., "Intelligent ship route planning via an A search model enhanced double-deep Q-network," Ocean Eng., vol. 327, pp. 120956, May. 2025.

[7] X. Luo, R. Yan, and S. Wang, "Ship sailing speed optimization considering dynamic meteorological conditions," Transp. Res. Part C: Emerg. Technol., vol. 167, pp. 104827, Oct. 2024.

[8] S. Zhou, Z. Guo, J. Chen, et al., "Large containership stowage planning for maritime logistics: A novel meta-heuristic algorithm to reduce the number of shifts," Adv. Eng. Inform., vol. 64, pp. 102962, Mar. 2025.

[9] M. K. Msakni, K. Fagerholt, F. Meisel, et al., "Analyzing different designs of liner shipping feeder networks: A case study," Transp. Res. Part E: Logist. Transp. Rev., vol. 134, pp. 101839, Feb. 2020.

[10] Y. Wang and S. Wang, "Deploying, scheduling, and sequencing heterogeneous vessels in a liner container shipping route," Transp. Res. Part E: Logist. Transp. Rev., vol. 151, pp. 102365, Jul. 2021.

[11] M. A. Dulebenets, "The vessel scheduling problem in a liner shipping route with heterogeneous fleet," Int. J. Civ. Eng., vol. 16, pp. 19–32, Oct. 2018.

[12] J. Pasha, M. A. Dulebenets, A. M. Fathollahi-Fard, et al., "An integrated optimization method for tactical-level planning in liner shipping with heterogeneous ship fleet and environmental considerations," Adv. Eng. Inform., vol. 48, pp. 101299, Apr. 2021.

[13] S. Zhao, H. Yang, J. Zheng, et al., "A two-step approach for deploying heterogeneous vessels and designing reliable schedule in liner shipping services," Transp. Res. Part E: Logist. Transp. Rev., vol. 182, pp. 103416, Feb. 2024.

[14] J. Du, K. Qin, R. Zhang, et al., "Multi-objective heterogeneous fleet deployment and scheduling with green technology adoption considered," Ocean Eng., vol. 311, pp. 118939, Nov. 2024.

[15] Y. Wang, H. Zhang, T. Wang, et al., "Heterogeneous vessel fleet co-management for liner alliances under profit-sharing agreement and weekly-dependent demand," Transp. Res. Part E: Logist. Transp. Rev., vol. 194, pp. 103880, Feb. 2025.

[16] H. Qiao, X. Lin, X. Zhou, et al., "Research on joint decision-making of timely delivery, product quality and marketing in supply chain based on differential game," Sustainability, vol. 14, pp. 10774, Aug. 2022.

[17] X. Liang, N. Wang, M. Zhang, et al., "Bi-objective multi-period vehicle routing for perishable goods delivery considering customer satisfaction," Expert Syst. Appl., vol. 220, pp. 119712, Jun. 2023.

[18] M. Huang, M. Liu, and H. Kuang, "Vehicle routing problem for fresh products distribution considering customer satisfaction through adaptive large neighborhood search," Comput. Ind. Eng., vol. 190, pp. 110022, Apr. 2024.

[19] X. Yu, Y. Li, J. Liu, et al., "Solving low-carbon last mile delivery problem using discrete marine predators algorithm," Appl. Soft Comput., vol. 165, pp. 112112, Nov. 2024.

[20] K. Seo and T. Roh, "Online and offline delivery qualities: O2O satisfaction and loyalty through technology acceptance model," J. Retail. Consum. Serv., vol. 82, pp. 104079, Jan. 2025.

[21] S. Maji, S. Maity, I. E. Nielsen, et al., "A multi-objective sustainable multipath delivery problem in hilly regions with customer-satisfaction using TLBO," Appl. Soft Comput., vol. 176, pp. 113100, May. 2025.

[22] S. Ropke and D. Pisinger, "An adaptive large neighborhood search heuristic for the pickup and delivery problem with time windows," Transp. Sci., vol. 40, pp. 455–472, Nov. 2006.

[23] X. Wang, Y. Liang, X. Wei, et al., "An adaptive large neighborhood search algorithm for the tugboat scheduling problem," Comput. Ind. Eng., vol. 177, pp. 109039, Mar. 2023.

[24] X. Wang, Y. Liang, E. P. Chew, et al., "Integrated optimization of pilot and pilot carrier routing in seaports," Comput. Oper. Res., vol. 171, pp. 106789, Nov. 2024.

[25] S. Zhang, J. Xia, Q. Chen, et al., "A two-phase adaptive large neighborhood search algorithm for the electric location routing problem with range anxiety," Appl. Soft Comput., vol. 167, pp. 112323, Dec. 2024.

[26] Y. Gao, L. Yang, M. Wang, et al., "Integrated energy scheduling under uncertainty for sustainable ports," Transp. Res. Part E: Logist. Transp. Rev., vol. 197, pp. 104033, May 2025.

[27] R. Özkır and E. Coban, "ALNS algorithm for load handling and AGV routing with trolleys," Comput. Ind. Eng., vol. 208, pp. 111334, Oct. 2025.

[28] F. Smarandache, Neutrosophy: Neutrosophic Probability, Set, and Logic. USA: American Research Press, 1998.

[29] H. Wang, F. Smarandache, Y. Q. Zhang, and R. Sunderraman, "Single valued neutrosophic sets," Multispace Multistruct., vol. 4, pp. 410–413, Apr. 2010.

[30] D. Kahneman and A. Tversky, "Prospect theory: An analysis of decision under risk," Econometrica, vol. 47, pp. 363–391, Mar. 1979.

[31] K. D. Edwards, "Prospect theory: A literature review," Int. Rev. Financ. Anal., vol. 5, pp. 19–38, 1996.

[32] S. F. Ghannadpour, S. Noori, R. Tavakkoli-Moghaddam, et al., "A multi-objective dynamic vehicle routing problem with fuzzy time windows: Model, solution and application," Appl. Soft Comput., vol. 14, pp. 504–527, Jan. 2014.

[33] J. Tang, Z. Pan, R. Y. K. Fung, et al., "Vehicle routing problem with fuzzy time windows," Fuzzy Sets Syst., vol. 160, pp. 683–695, Mar. 2009.

[34] C. Liu, Y. Zhou, Z. Yang, et al., "Optimizing the scheduling scheme for NSR/SCR tramp vessel shipping between Asia and Europe," Ocean Eng., vol. 304, pp. 117747, Jul. 2024.

[35] S. Wang and Q. Meng, "Sailing speed optimization for container ships in a liner shipping network," Transp. Res. Part E: Logist. Transp. Rev., vol. 48, pp. 701–714, May. 2012.

[36] M. A. Dulebenets, "A comprehensive multi-objective optimization model for the vessel scheduling problem in liner shipping," Int. J. Prod. Econ., vol. 196, pp. 293–318, Feb. 2018.

[37] P. Shaw, "Using constraint programming and local search methods to solve vehicle routing problems," in Proc. Int. Conf. Principles Practice Constraint Programming (CP98), Pisa, Italy, Oct. 1998, vol. 1520, pp. 417–431.

[38] Y. Shi, W. Liu, and Y. Zhou, "An adaptive large neighborhood search based approach for the vehicle routing problem with zone-based pricing," Eng. Appl. Artif. Intell., vol. 124, pp. 106506, Sep. 2023.

[39] J. Xie, B. Wu, and W. Zou, "Ordered weighted utility distance operators and their applications in group decision-making," Appl. Soft Comput., vol. 150, pp. 111016, Jan. 2024.

[40] P. He, J. G. Jin, W. Pan, et al., "Route, speed, and bunkering optimization for LNG-fueled tramp ship with alternative bunkering ports," Ocean Eng., vol. 305, pp. 117957, Aug. 2024.

[41] F. Yang and F. Tao, "A bi-objective optimization VRP model for cold chain logistics: Enhancing cost efficiency and customer satisfaction," IEEE Access, vol. 11, pp. 127043–127056, Nov. 2023.